全金属纳米结构制备及其在表面等离激元中的应用

报告人：朱新利
导师：俞大鹏教授
合作：张家森教授

北京大学物理学院
介观物理国家重点实验室

萃英研究生学术沙龙
2010.11.10

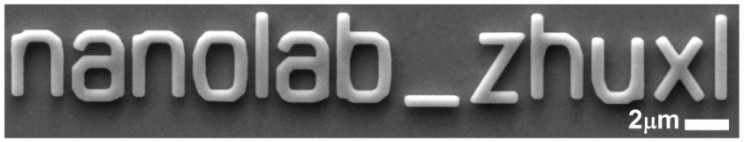

outline

1. 实验室简介
2. 全金属纳米结构制备工艺
3. 阴极荧光系统
4. 表面等离激元纳米腔模式研究

俞大鹏团队实验室简介

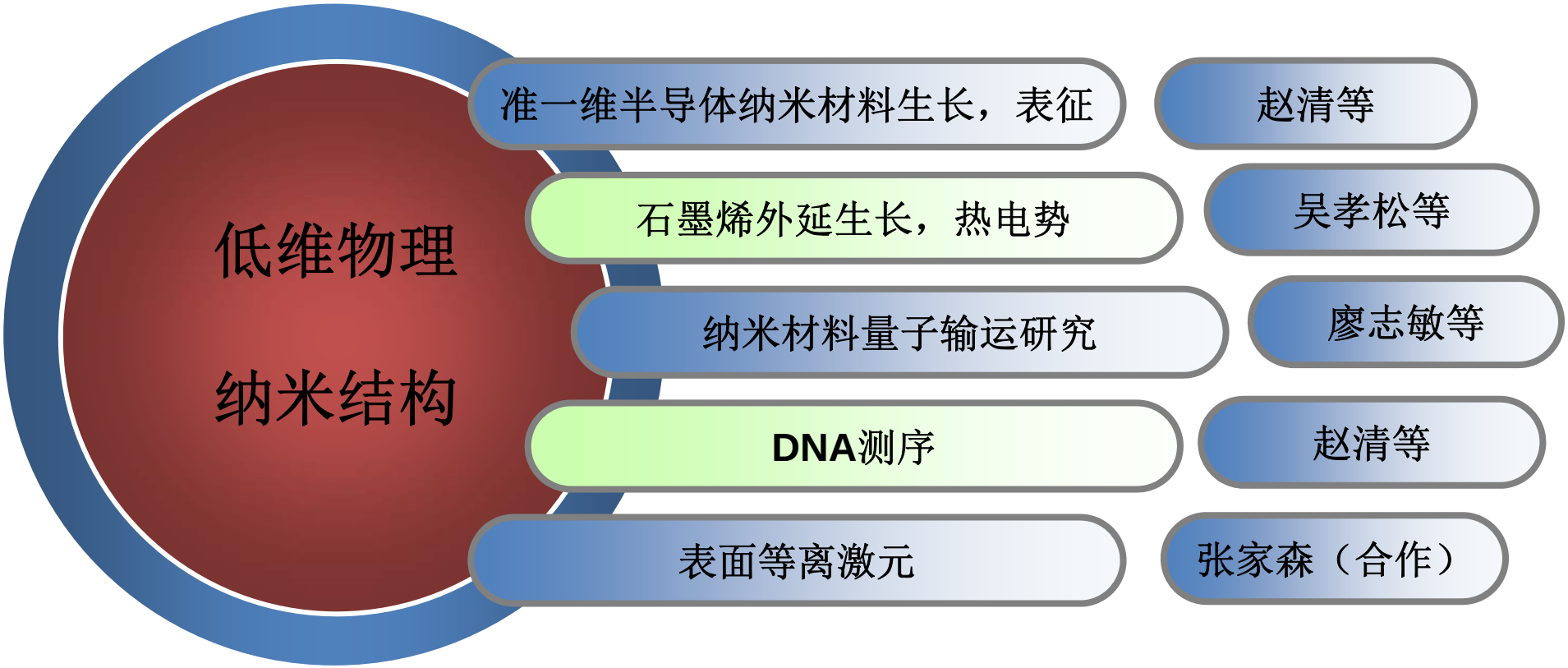
低维物理
纳米结构
准一维半导体纳米材料生长，表征
赵清等
石墨烯外延生长，热电势
吴孝松等
纳米材料量子输运研究
廖志敏等
DNA测序
赵清等
表面等离激元
张家森（合作）

北京大学电子显微镜实验室简介 http://eml.pku.edu.cn/index.aspx

主任：俞大鹏　副主任：徐军

扫描电子显微镜组

Quanta 200F 环境扫描电子显微镜	负责人：陈莉
Strata DB 235型FIB双束系统 （Raith EBL）	负责人：徐军
Nano 430 扫描电子显微镜	负责人：张会珍

透射电子显微镜组

Technai T20　透射电子显微镜	负责人：李雪梅
H 9000 透射电子显微镜	负责人：陈晶
Technai F20　透射电子显微镜	负责人：张敬民
Technai F30　透射电子显微镜	负责人：尤力平

outline

1. 实验室简介
2. 全金属纳米结构制备工艺
3. 阴极荧光系统
4. 表面等离激元纳米腔模式研究

Various fabrication method (traditional)

Focus Ion beam(FIB) milling

Nanosphere Lithography (NSL)

Electron Beam Lithography (EBL)

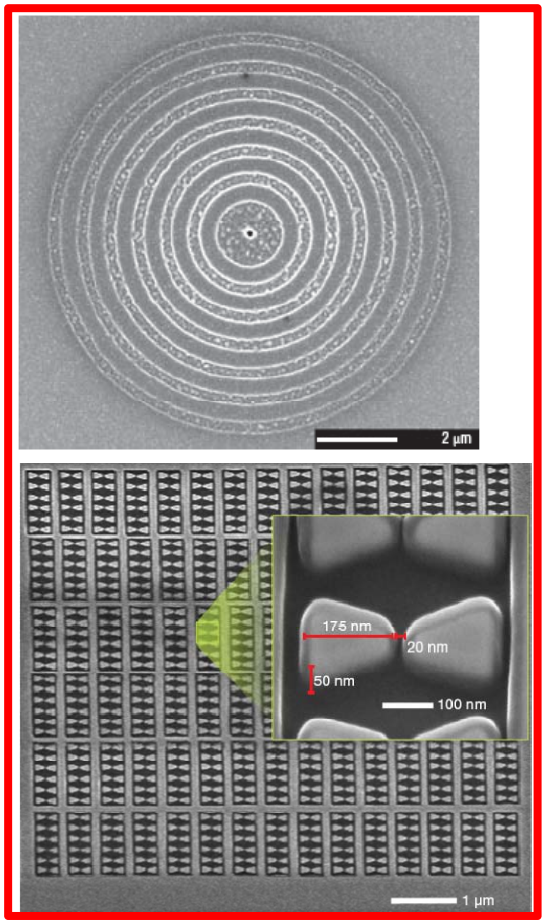

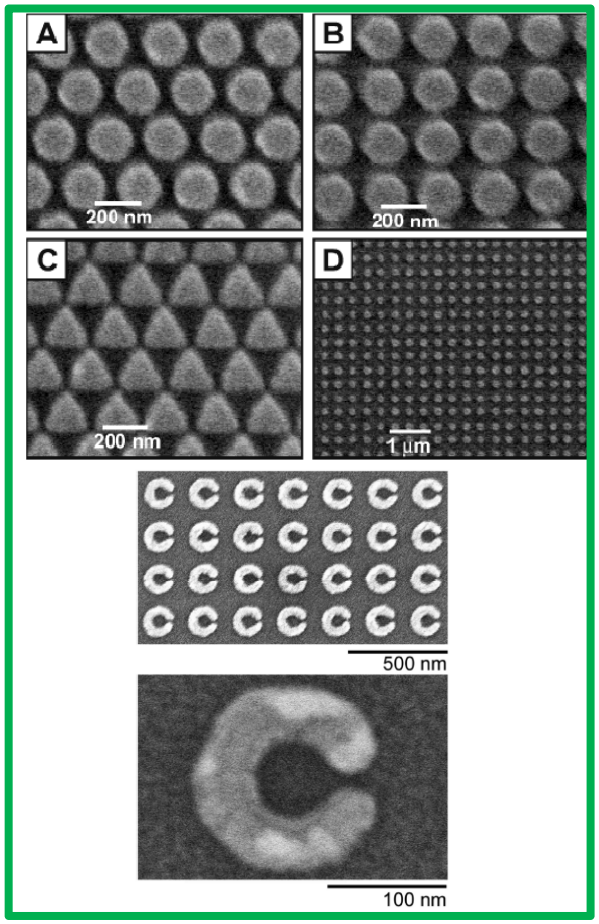

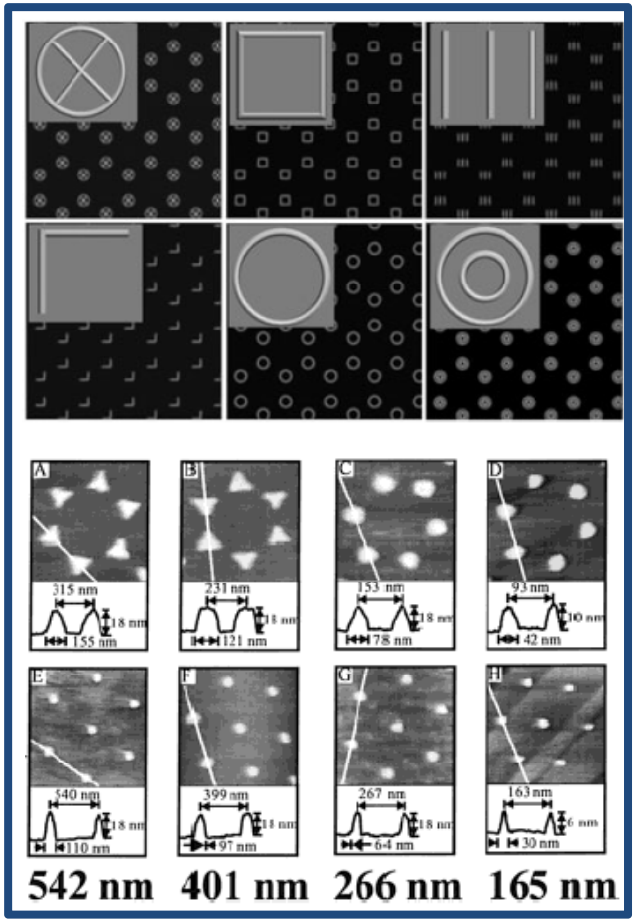

1. Nature, 453, 757; Nature Photonics, 2, 161.
2. J. Phys. Chem. B 107, 30; J. Am. Chem. Soc. 131, 1761.
3. J. Phys. Chem. B 105, 5599; Small 2005, 1, No. 4, 439.

Our method

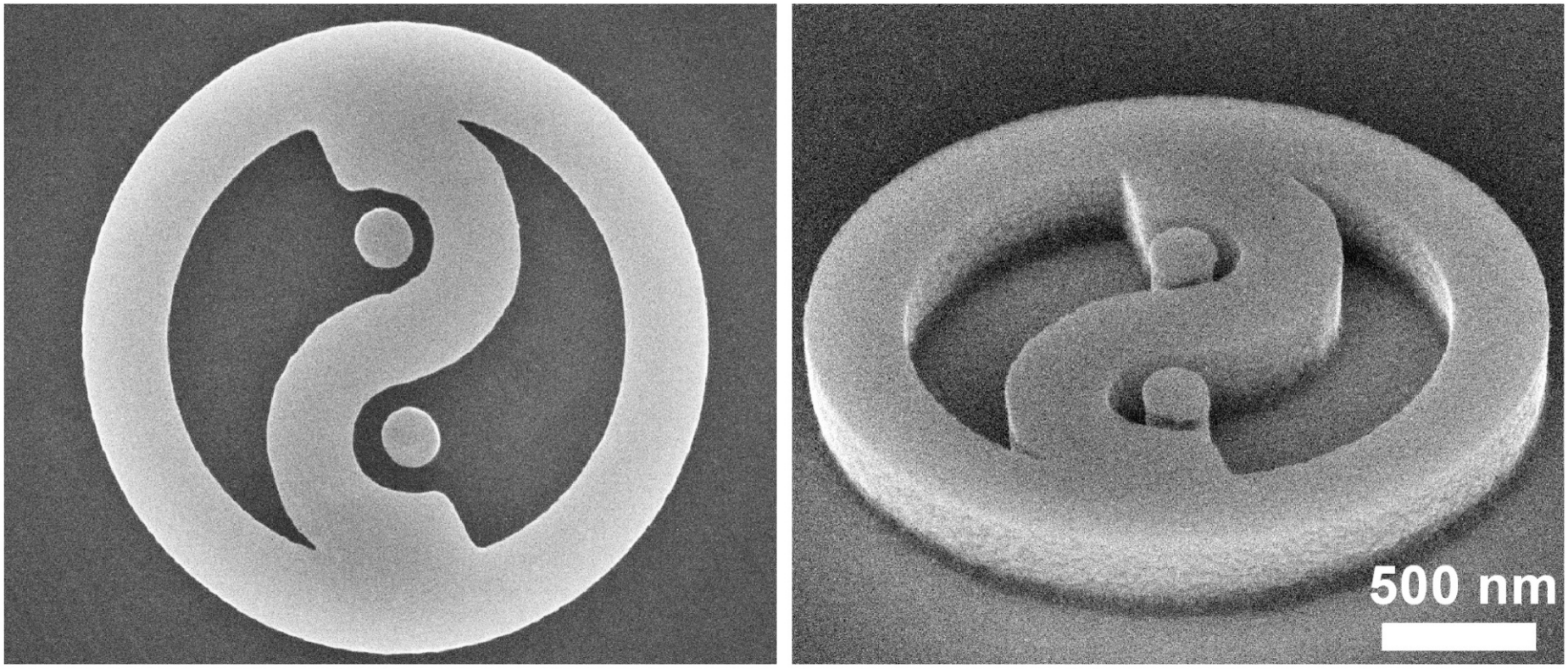

ultrasmooth surface,
high aspect ratio,
controllable shapes and sizes(complex)

Fabrication process: PMMA-based template stripping method

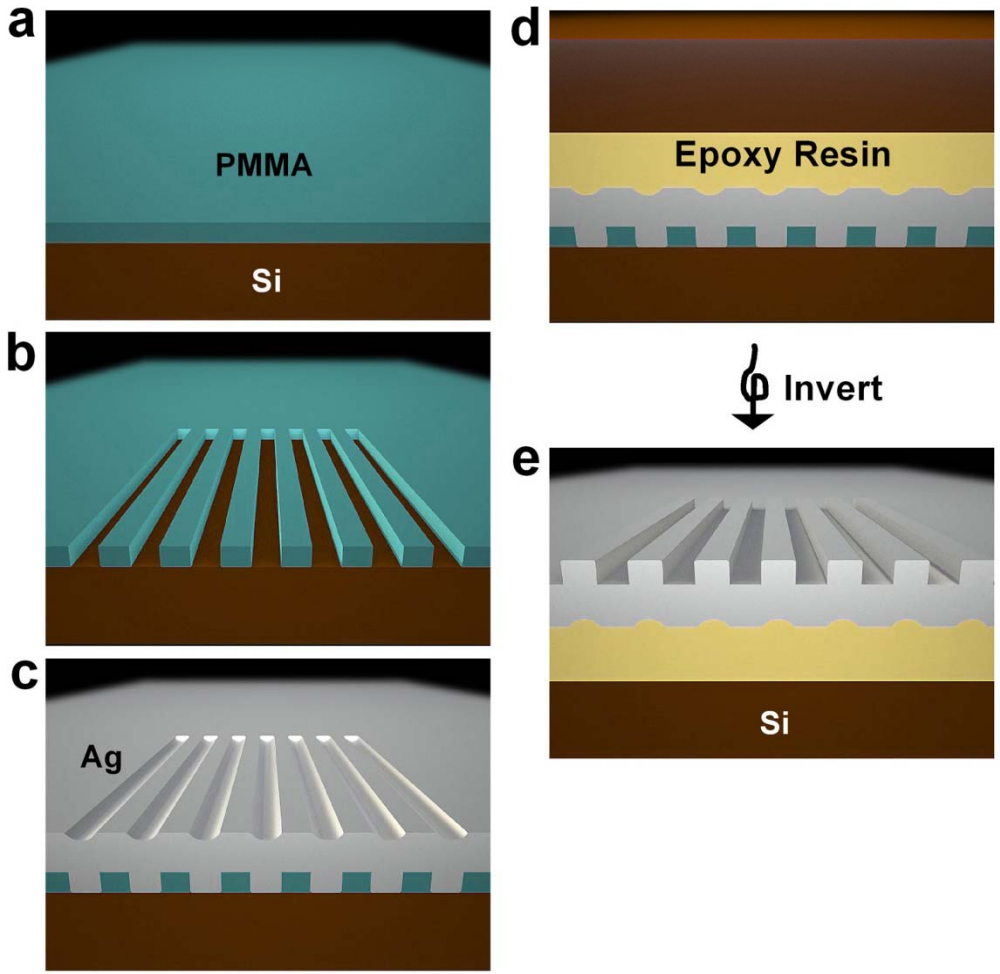

Schematic diagram of the fabrication process

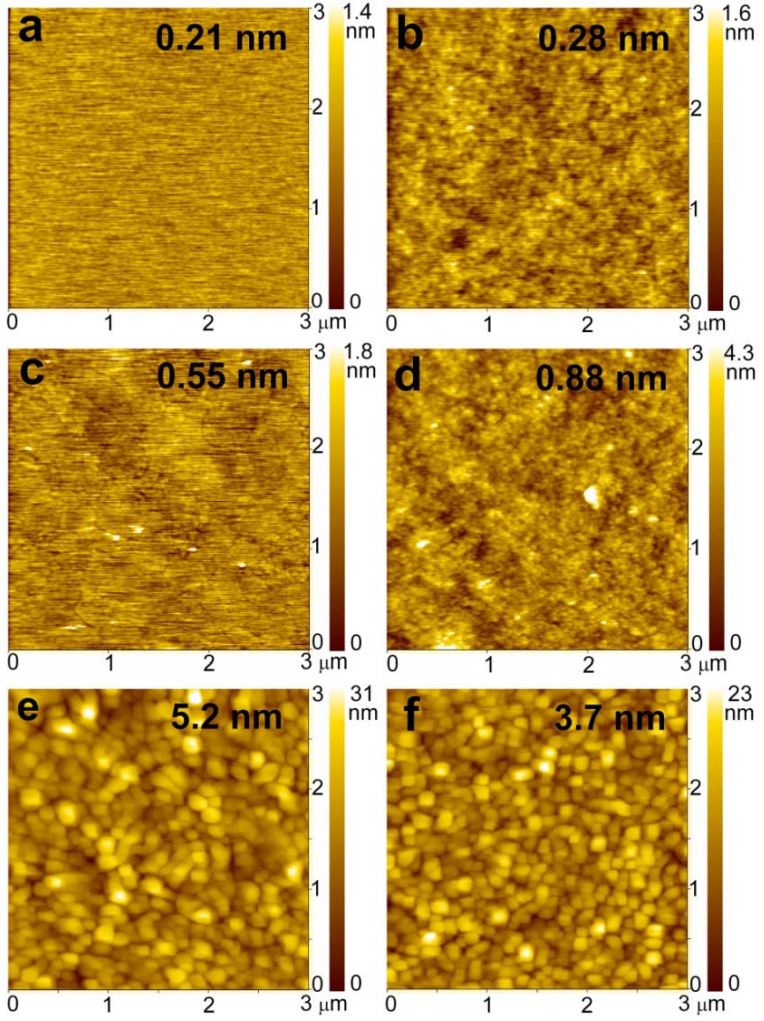

AFM measurement

Xinli Zhu *et al*., DOI: 10.1002/adma.201001313

Typical SEM images of various silver nanostructures

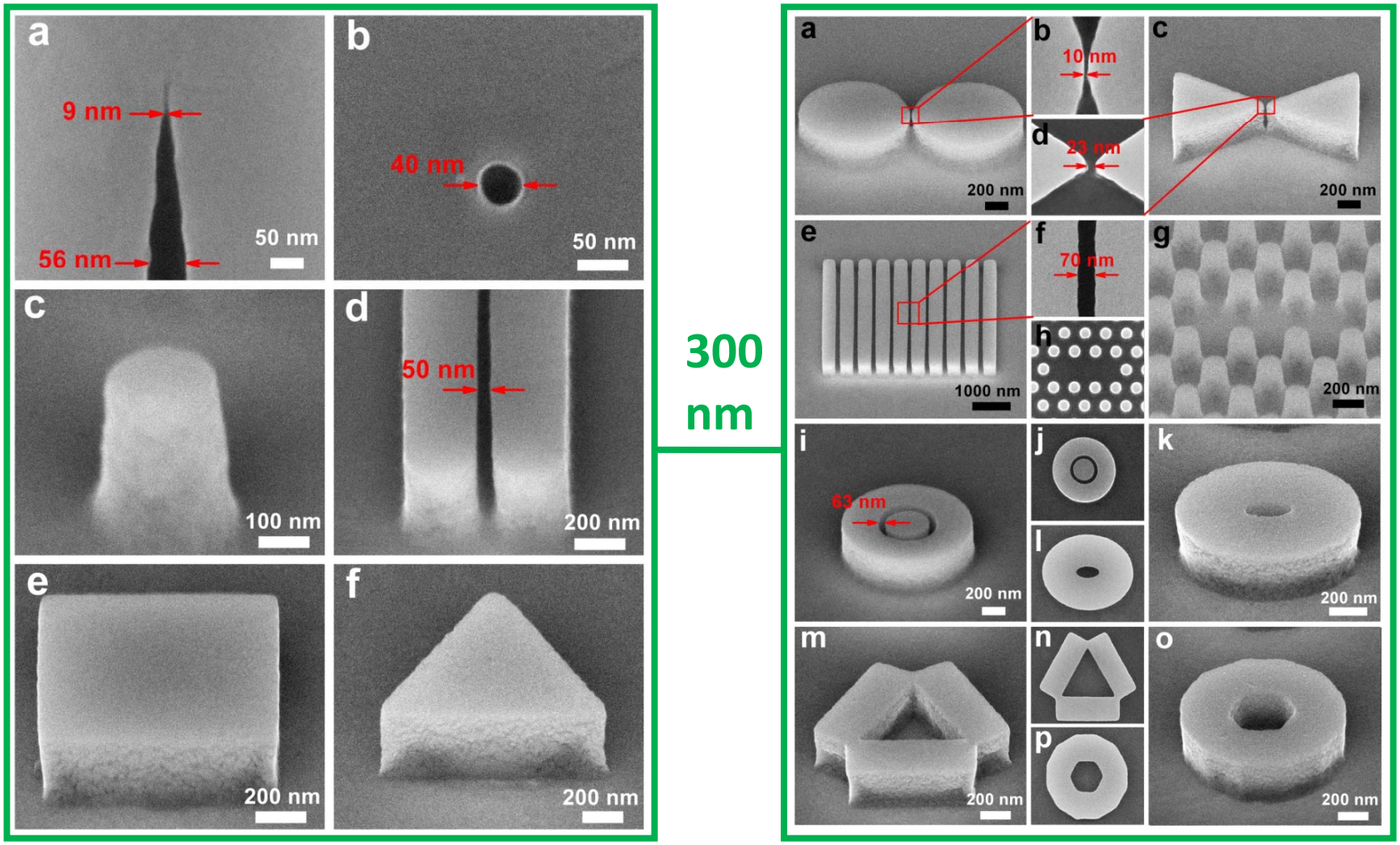

SPPs: excite, guide, focuse, confine

Xinli Zhu *et al*., DOI: 10.1002/adma.201001313

More…

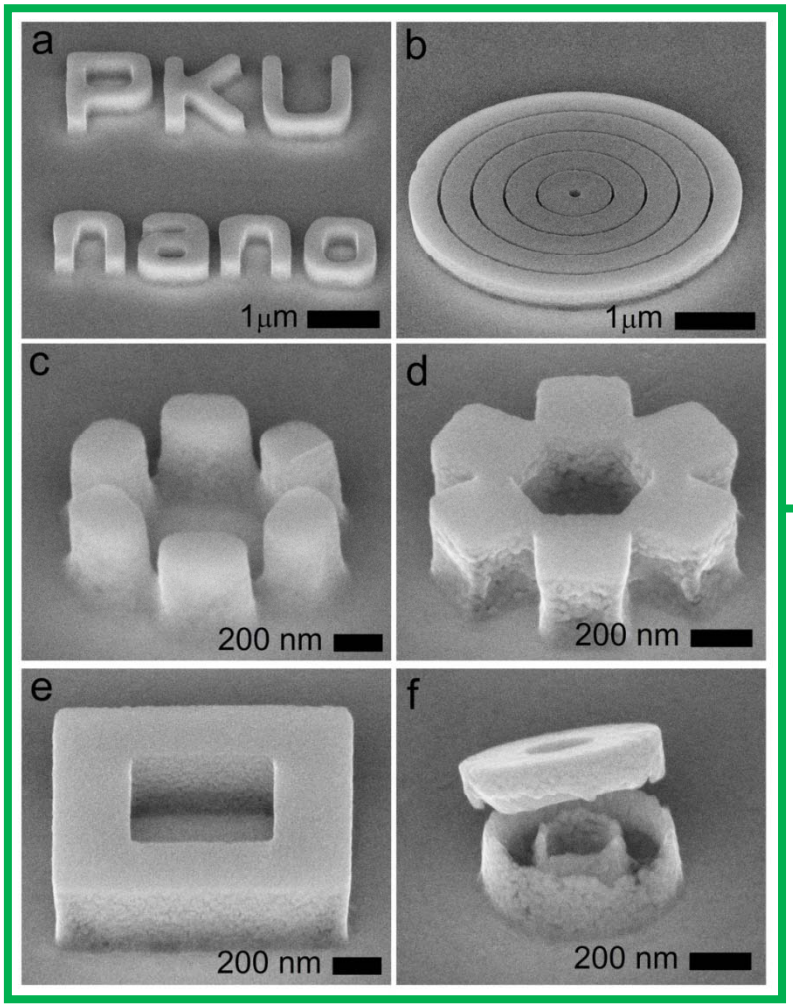
a
PKU
nano
1μm
b
1μm
c
200 nm
d
200 nm
e
200 nm
f
200 nm

300 nm

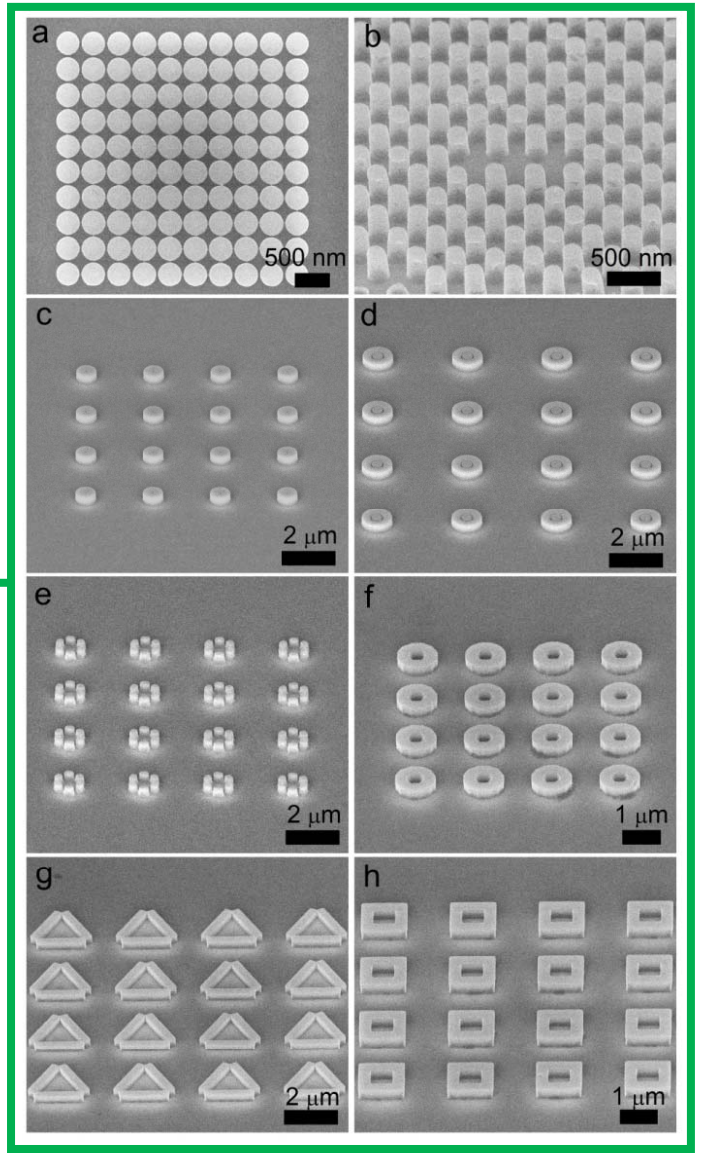
a
500 nm
b
500 nm
c
2 μm
d
2 μm
e
2 μm
f
1 μm
g
2 μm
h
1 μm

Height: 60 and 700 nm

60 nm

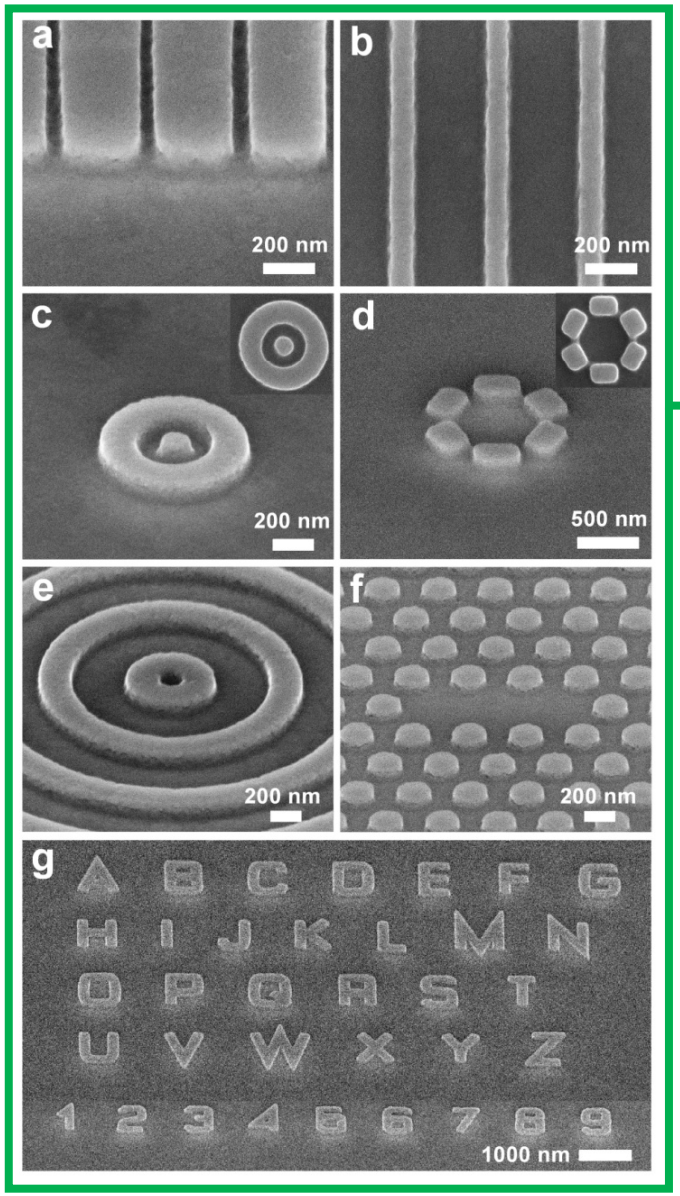

700 nm

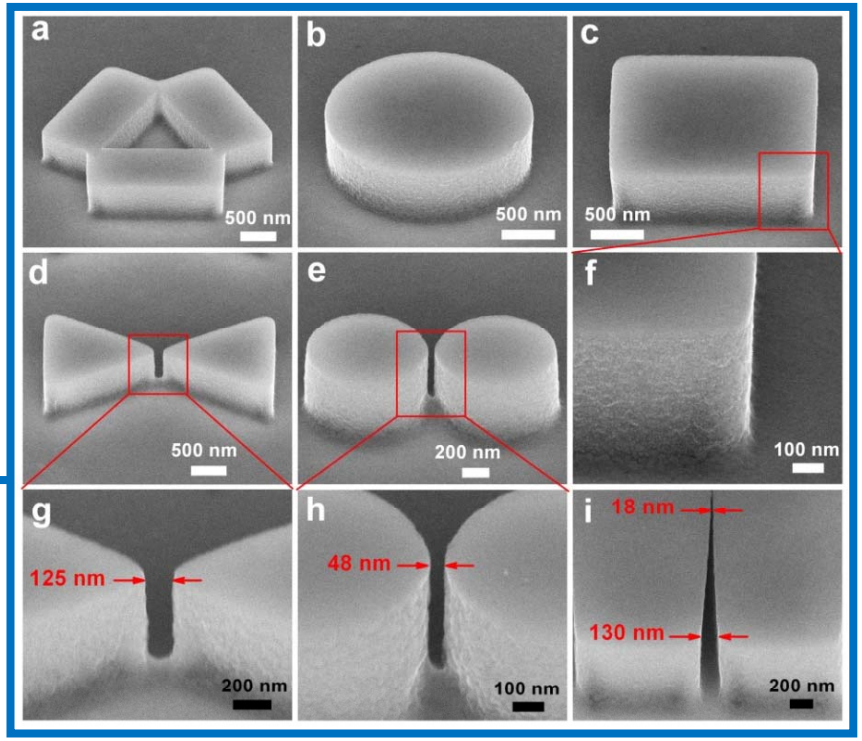

3D shape and size controllable

outline

1. 实验室简介
2. 全金属纳米结构制备工艺
3. 阴极荧光系统
4. 表面等离激元纳米腔模式研究

Surface plasmon polaritons (SPPs)

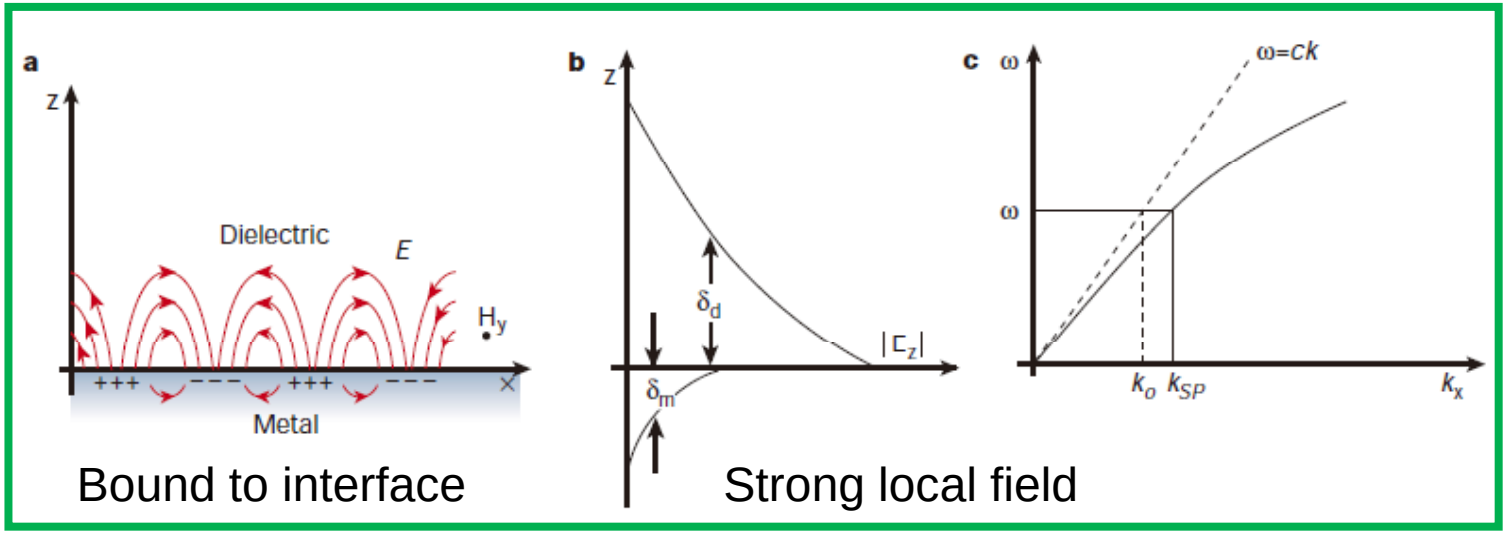

transverse magnetic wave

$$k_{\mathrm{p}} = \frac{\omega}{c}\left(\frac{\varepsilon_{\mathrm{d}}\varepsilon_{\mathrm{m}}}{\varepsilon_{\mathrm{d}}+\varepsilon_{\mathrm{m}}}\right)^{1/2} = \frac{\omega}{c}\varepsilon_{2\mathrm{D}}^{1/2}$$

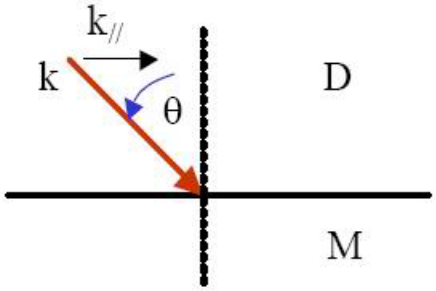

$$k_{sp} = k_x \pm nG_x \pm mG_y$$

$$k_x = \frac{2\pi}{\lambda}\sin\theta$$

$$G_x = \frac{2\pi}{a_{0x}}, \quad G_y = \frac{2\pi}{a_{0y}}$$

Nature, 424,824 (2003).

Optical excitations in electron microscopy

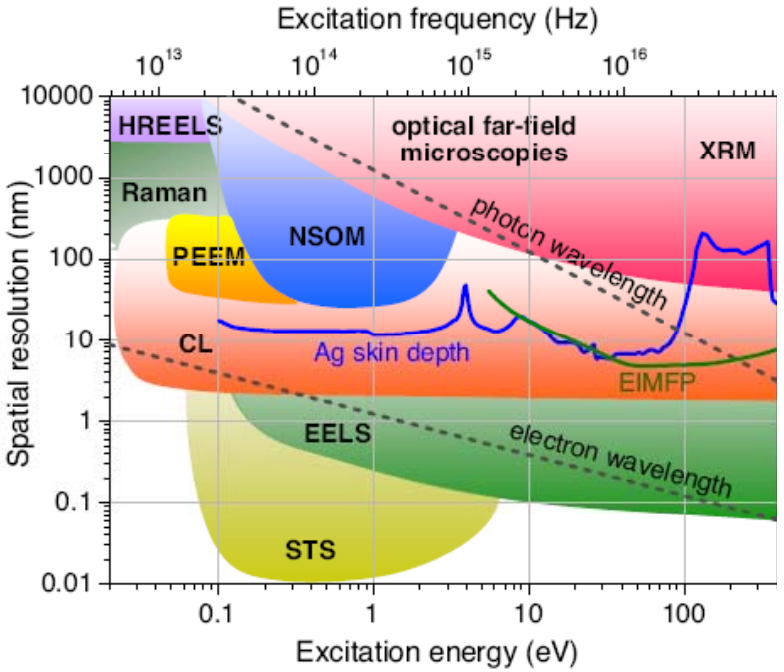

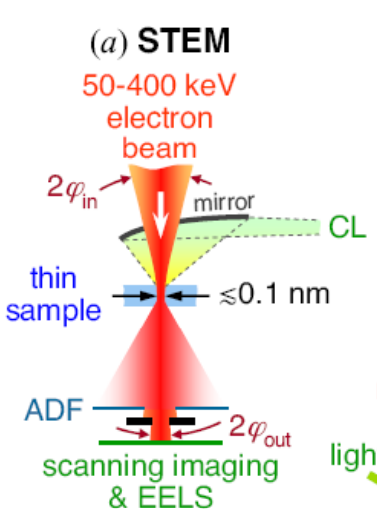

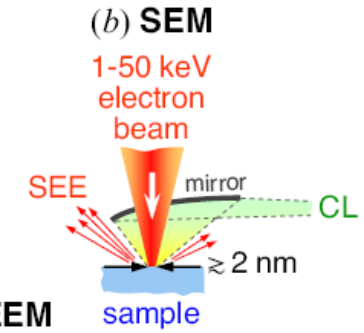

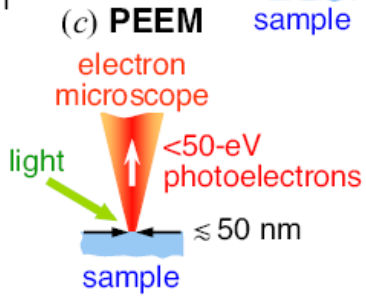

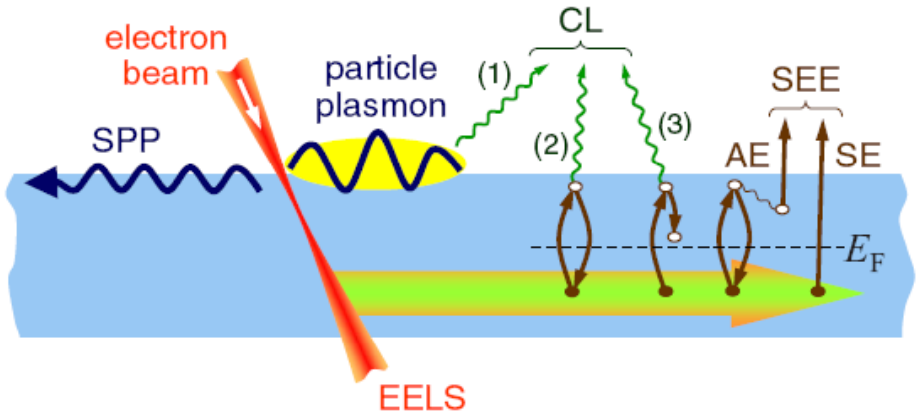

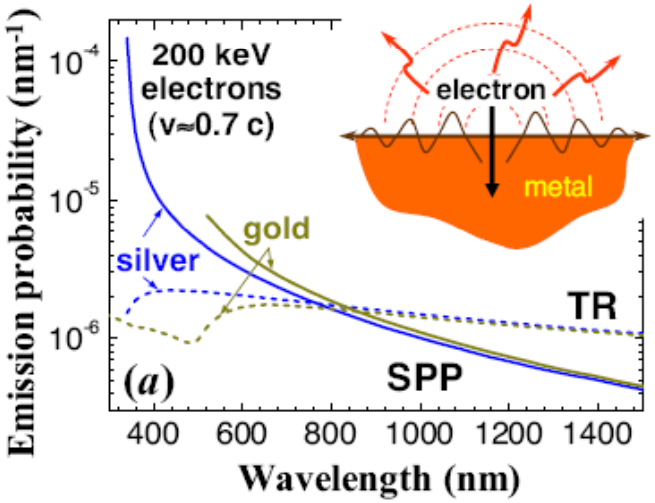

Rev. Mod. Phys., Vol. 82, No. 1, January–March 2010

Optical excitations in electron microscopy

	Structure	Technique	$\hbar\omega$ (eV)	Reference	Comments
SP	Al planar surfaces	REELS	5–100	Powell and Swan, 1959	Observation of planar SPs
SPP	Al gratings	CL	2.3	Teng and Stern, 1967	SPP signature in CL
LPR	Al nanoparticles	CL	3–8	Fujimoto and Komaki, 1968	Mie modes
SPP	Al films	EELS	2–12	Pettit *et al.*, 1975	SPP dispersion
SP	Al and In surfaces	EELS	8–12	Krane and Raether, 1976	Large-q dispersion
SPP	Ag shallow grating	CL	2–3	Heitmann, 1977	SPP dispersion
LPR	Al nanospheres	EELS	1–20	Batson, 1980	Size dependence of LPR
LPR	Al spheres on AlO_3	EELS	1–40	Wang and Cowley, 1987a	Plasmon maps
LPR	Al spheres on Al	EELS	1–40	Wang and Cowley, 1987a	Plasmon maps
LPR	Ag nanospheres	EELS	3–5	Ouyang *et al.*, 1992	Nonlocal effects
LPR	Si nanospheres	EELS	2–35	Ugarte *et al.*, 1992	Plasmon maps
LPR	Al nanospheres	EELS	2–40	Stöckli *et al.*, 1997	
SP	Al_2O_3 nanospheres	EELS	2–30	Abe *et al.*, 2000	Radiation losses
SPP	Ag gratings	CL	1–4	Yamamoto, Araya, Toda, and Sugiyama, 2001	Plasmon standing waves
LPR	Ag nanospheres	CL	2–4	Yamamoto, Araya, and García de Abajo, 2001	Plasmon maps of Mie modes
LPR	WS_3 nanotubes	EELS	3–30	Kociak *et al.*, 2001	
LPR	C nanotubes	EELS	3–30	Stéphan *et al.*, 2002	π and σ plasmons
LPR	Ag rough gratings	PEEM	3	Kubo *et al.*, 2005	Femtosecond dynamics
SPP	Au planar surfaces	CL	1–3	Bashevoy *et al.*, 2006 van Wijngaarden *et al.*, 2006	SPP propagation
LPR	Ag sphere dimer	CL	2–4	Yamamoto, Nakano, and Suzuki, 2006	Plasmon maps
LPR	Ag nanowires	CL	1–4	Yamamoto, Nakano, and Suzuki, 2006	Plasmon maps
SPP	Au atom wire array	LEEM	0.1–0.8	Nagao *et al.*, 2006	1D plasmon dispersion
LPR	Ag nanotriangles	EELS	1–4	Nelayah, Kociak, *et al.*, 2007	Plasmon maps
LPR	Ag nanowires	CL	1–4	Vesseur *et al.*, 2007	Plasmon maps
SPP	Au planar surfaces	CL	1–3	Bashevoy *et al.*, 2007	Hyperspectral imaging
SPP	Ag steps	PEEM	3	Kubo *et al.*, 2007	Femtosecond dynamics
LPR	Au annular grating	CL	1–3	Hofmann *et al.*, 2007	Plasmon maps
SP	HfO_2 in stacks	EELS	2–50	Couillard *et al.*, 2007	Multilayer plasmons
SP	$Si/SiO_2/Si$ stacks	EELS	2–50	Couillard *et al.*, 2008	
SPP	Au planar surfaces	CL	1–3	Kuttge *et al.*, 2008 Peale *et al.*, 2008 Yamamoto and Suzuki, 2008	SPP propagation
SPP	Au structured surfaces	CL	1–3	Kuttge, Vesseur, and Polman, 2009	SPP confinement
LPR	Au ridge	CL	1–3	Vesseur *et al.*, 2008	Plasmon maps
LPR	Au rods, spheres, ellipsoids, dimers, and touching dimers	EELS	1–4	Bosman *et al.*, 2007 N'Gom *et al.*, 2008 Chu *et al.*, 2009 Schaffer *et al.*, 2009	Plasmon maps and spectra

Rev. Mod. Phys., Vol. 82, No. 1, January–March 2010

Mapping surface plasmons via cathodoluminescence spectroscopy

Gatan MonoCL3+
detection system

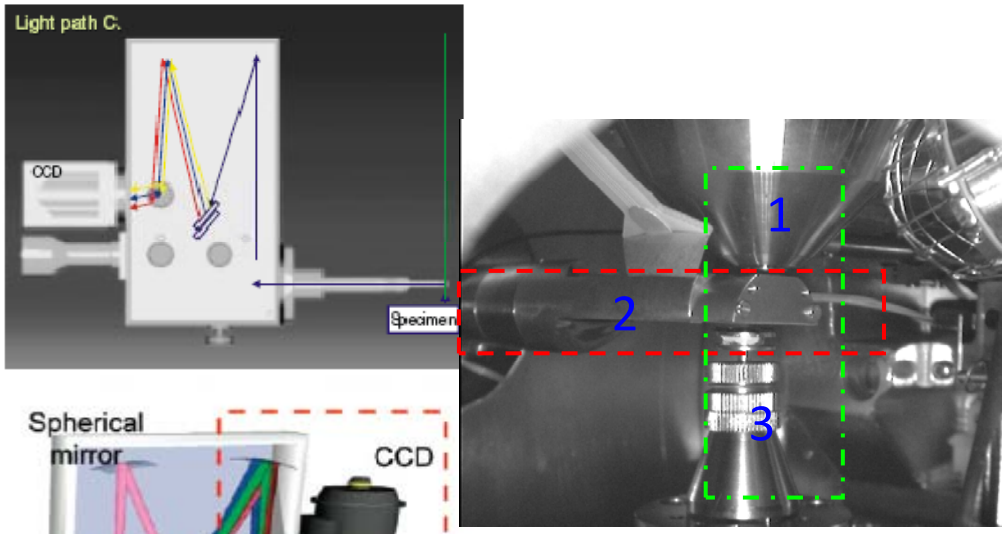

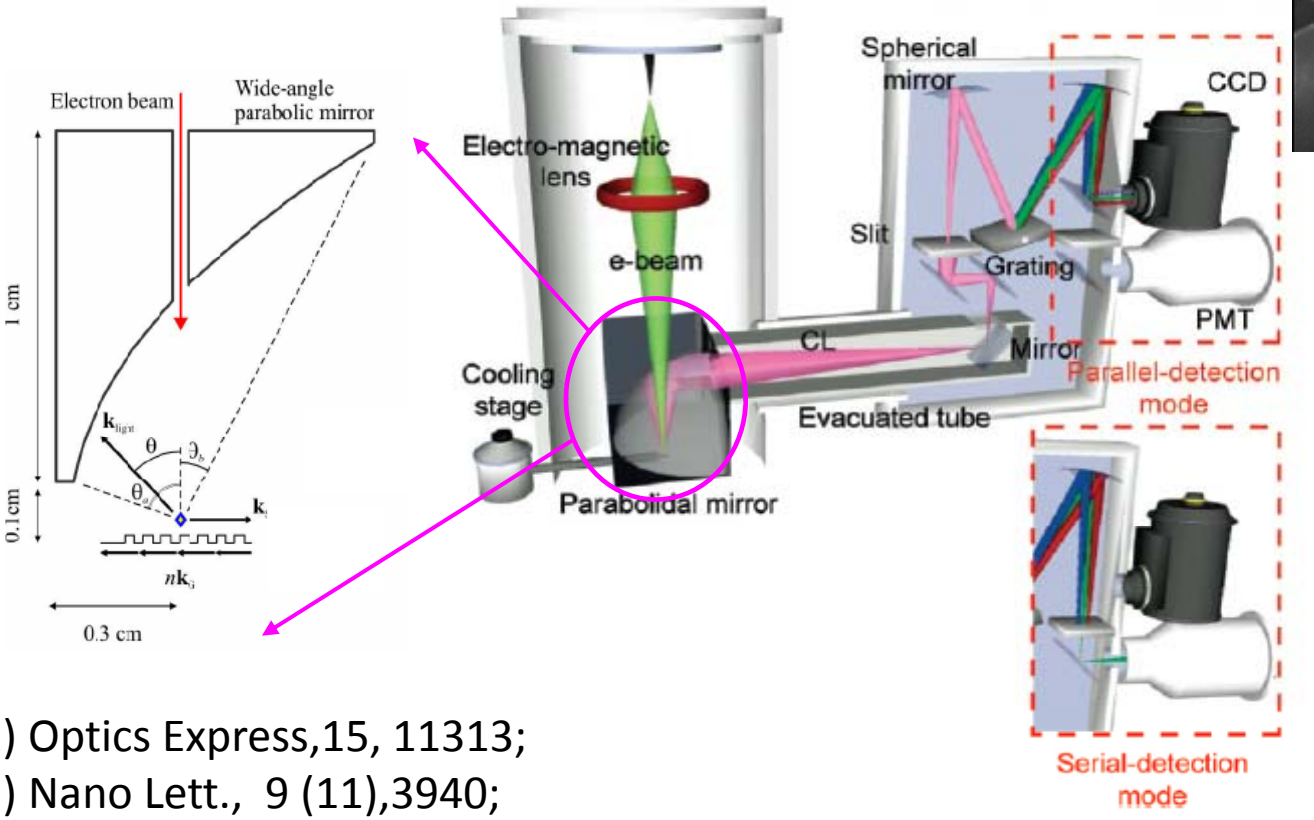

FEI Quanta 200 F
30keV

1) Optics Express,15, 11313;
2) Nano Lett., 9 (11),3940;
3) Phys. Stat. Sol. (c) 0,1028.

Mapping surface plasmons via cathodoluminescence spectroscopy

What CL monochromatic images represent ?

1) The intensity of each pixel represents the photon rate measured when the electron beam is positioned at that spot of the sample. This imaging technique is similar to SEM mapping, except that we use the light intensity collected by the ellipsoidal mirror rather than secondary electrons.
2) Mapping reveals the efficiency with which electron energy is coupled to far-field radiation as a function of electron injection position and not the distribution of light emission; i.e., while the electron-beam excitation is confined to a nanoscale spot, the associated optical emission may come from any part of the structure.

$10/(1024 \times 943)s \approx 1\mu s >> T_{spp}$

Without delay

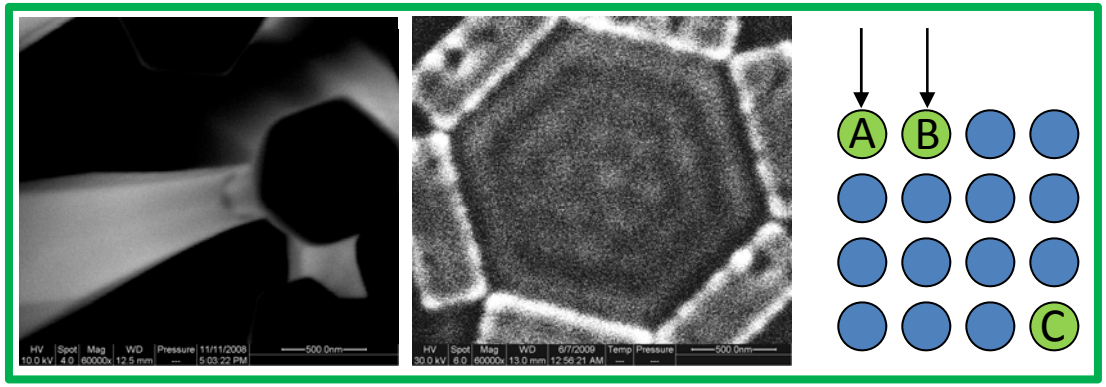

outline

1. 实验室简介
2. 全金属纳米结构制备工艺
3. 阴极荧光系统
4. 表面等离激元纳米腔模式研究

CL spectra and mode patterns of the boxing ring-shaped cavities

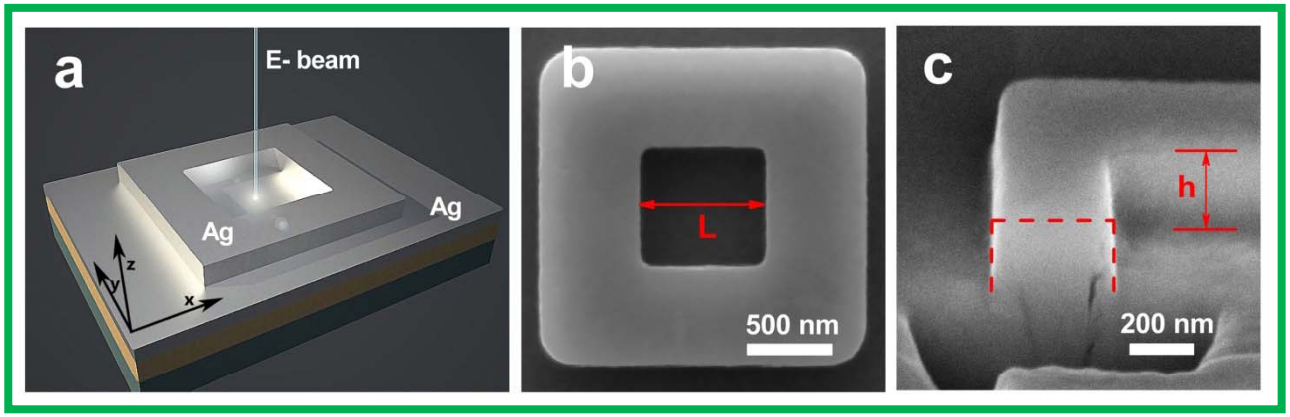

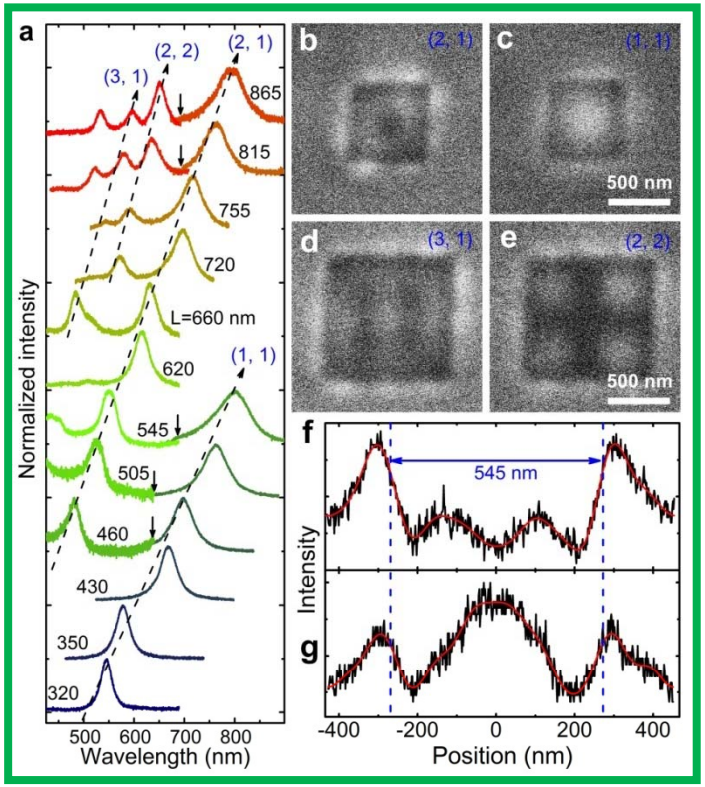

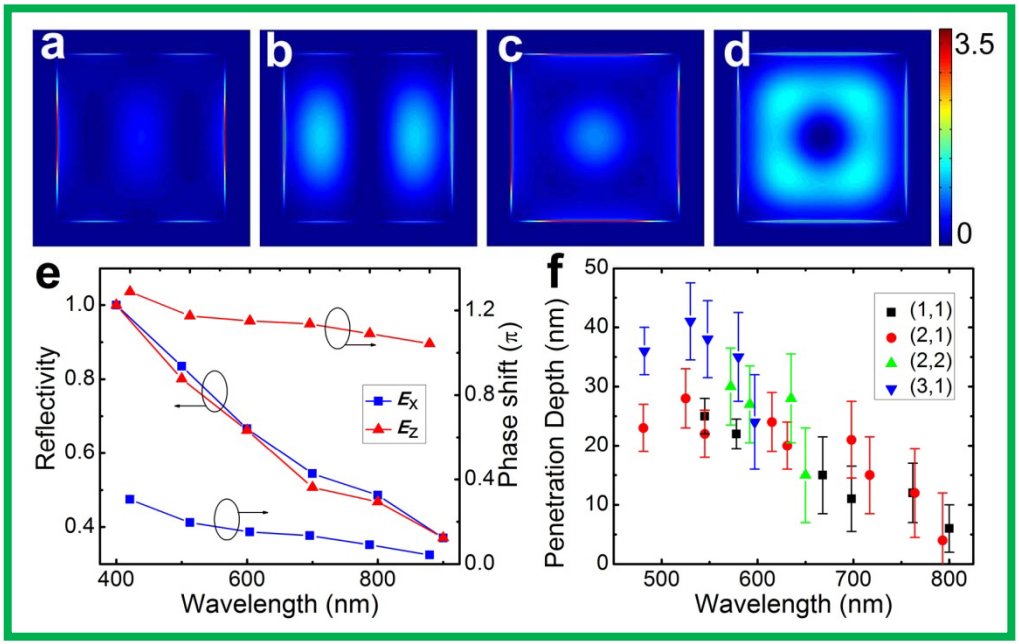

Xinli Zhu *et al*., Physical Review Letters 105,127402 (2010)

Quality factor(Q-factor) and Modal volume

The Q-factor of a cavity is determined by the energy loss per cycle versus the energy stored.

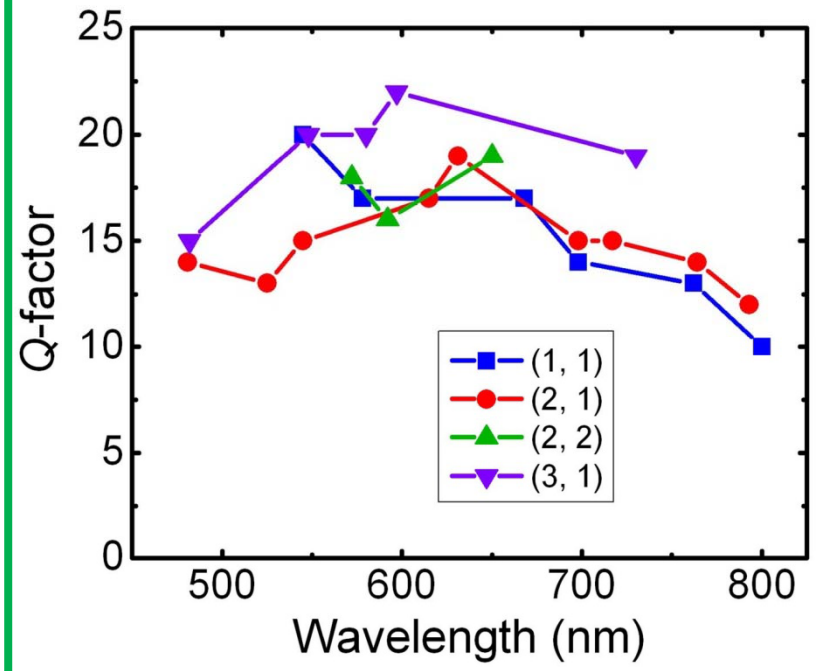

Resonant condition of the nanocavity:

$$L + 2\delta(\lambda_{SPP}) = \sqrt{m^2 + n^2} \cdot \frac{\lambda_{SPP}}{2}$$

Modal volume:

$$V = \lambda_{SPP}^3 \left(1 + \left|\varepsilon_m^{'}\right|\right)\left(32\pi\sqrt{\left|\varepsilon_m^{'}\right|}\right)^{-1}$$

for (1,1) mode

Experiment: L= 320 nm

λ = 545 nm

$V = 0.035\lambda^3_{spp} = 0.0049\ \mu m^3$

Xinli Zhu *et al*., Physical Review Letters 105,127402 (2010)

Q/V

namely, enabling enhanced strong light matter interactions.

High Q/ V ratio is important in increasing light-matter interactions in processes such as spontaneous emission, nonlinear optical processes and strong coupling.

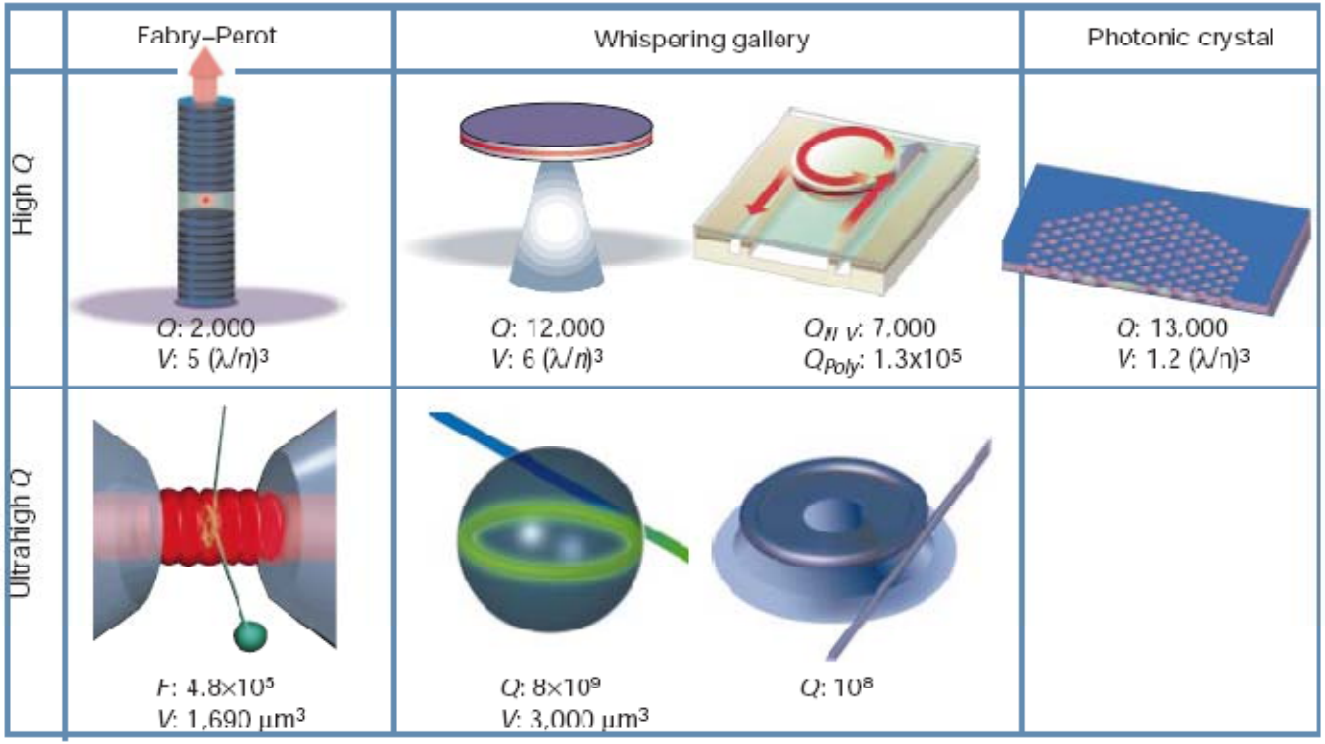

284	2.7x10^6	**Our case ~ 4000**

Nature, 424,839.

Optics express, 16,17690.

CL spectra and mode patterns of the boxing ring-shaped cavities

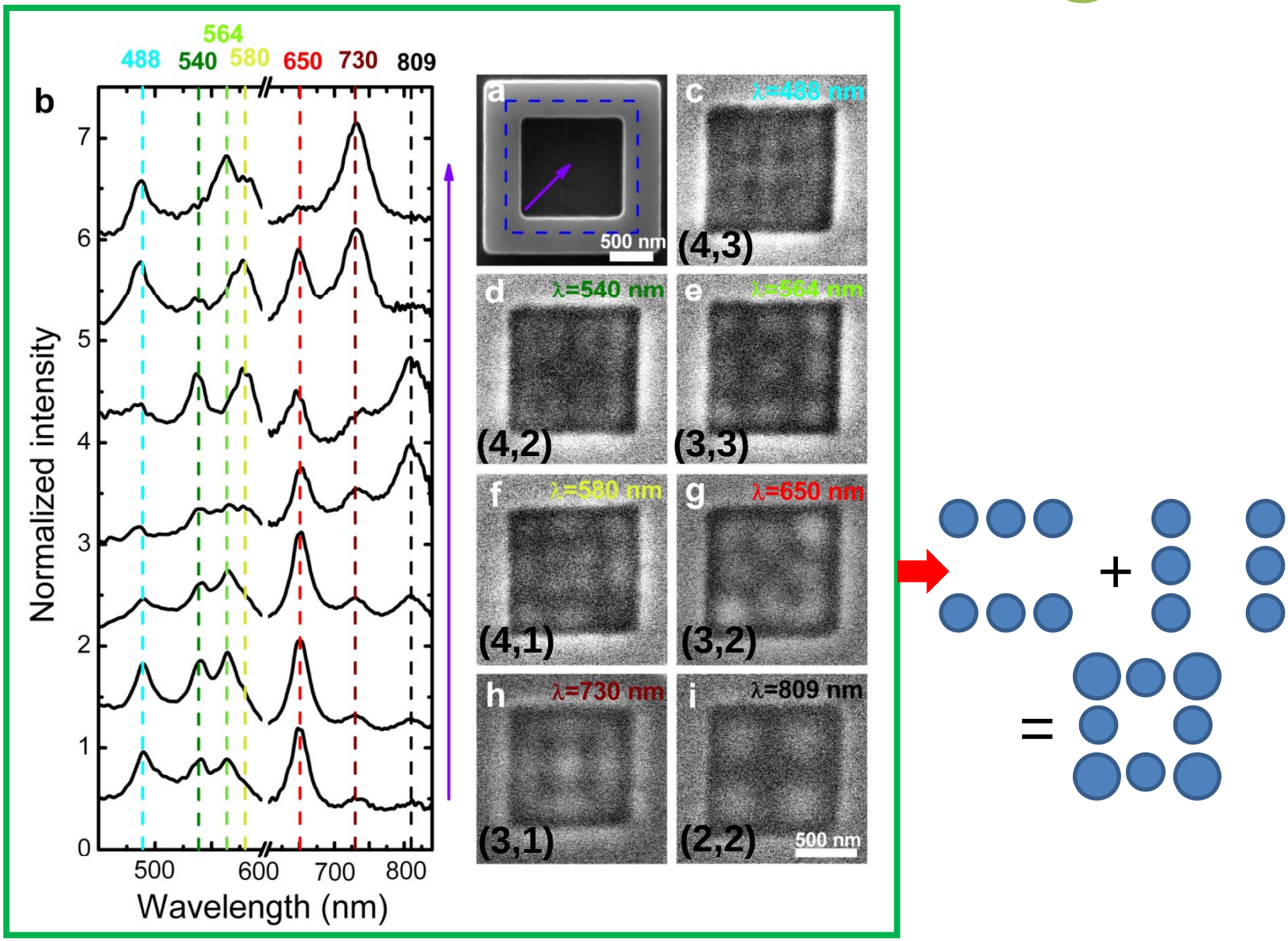

Xinli Zhu *et al.*, Physical Review Letters 105,127402 (2010)

CL spectra and mode patterns of the equilateral-triangle cavities

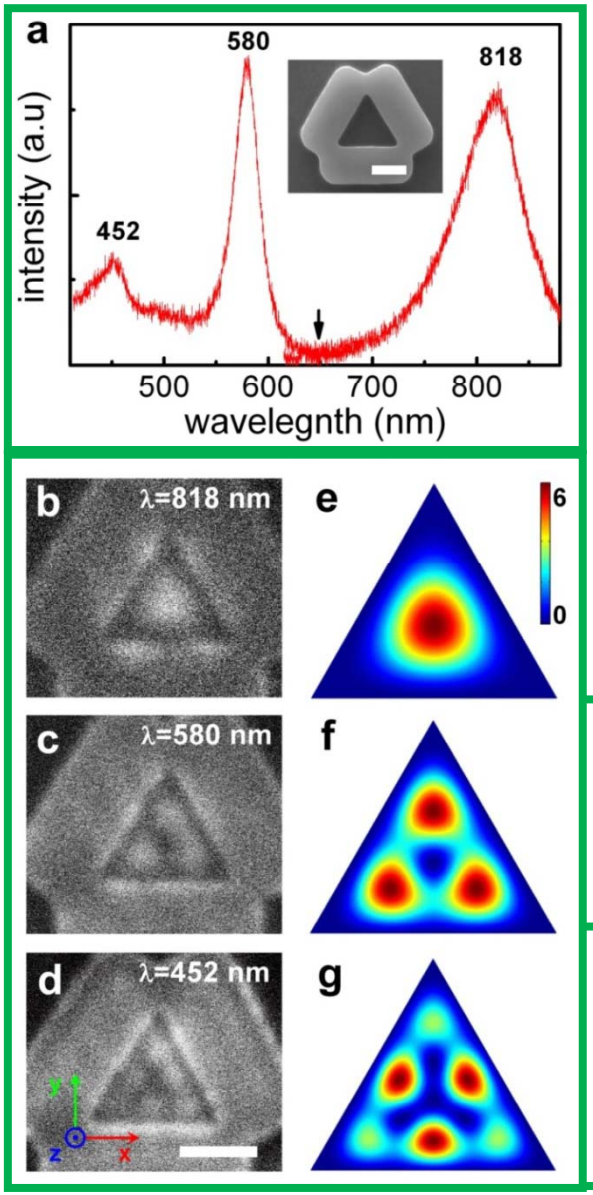

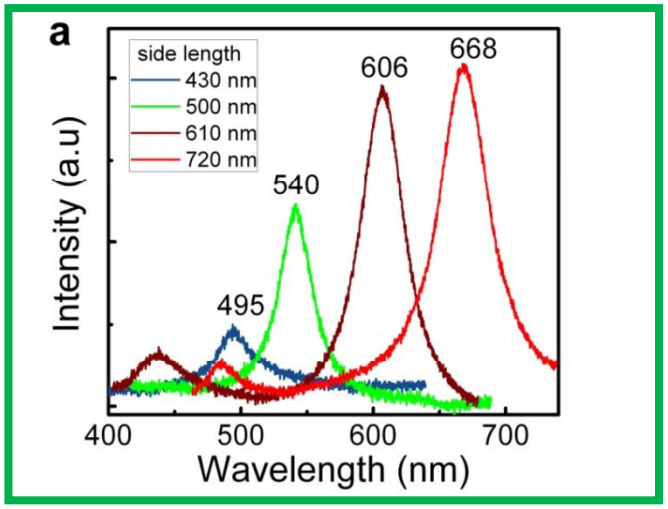

(1,3)

degeneration mode of **(1,5) and (2,4)**

degeneration mode of **(1,7)** and **(3,5)**

Xinli Zhu *et al*., DOI: 10.1002/adma.201001313

How to understand the resonant behavior of the cavity?

Maxwell equations

$$(\nabla^2+\mu\varepsilon k^2)\,\psi=0$$

Wave vector $\boldsymbol{K}_1$; Wave function：

$$e^{ik_1x}$$

$$e^{-ik_1[(x+a)/2-\sqrt{3}y/2]}$$

$$e^{-ik_1[(x-a)/2+\sqrt{3}y/2]}$$

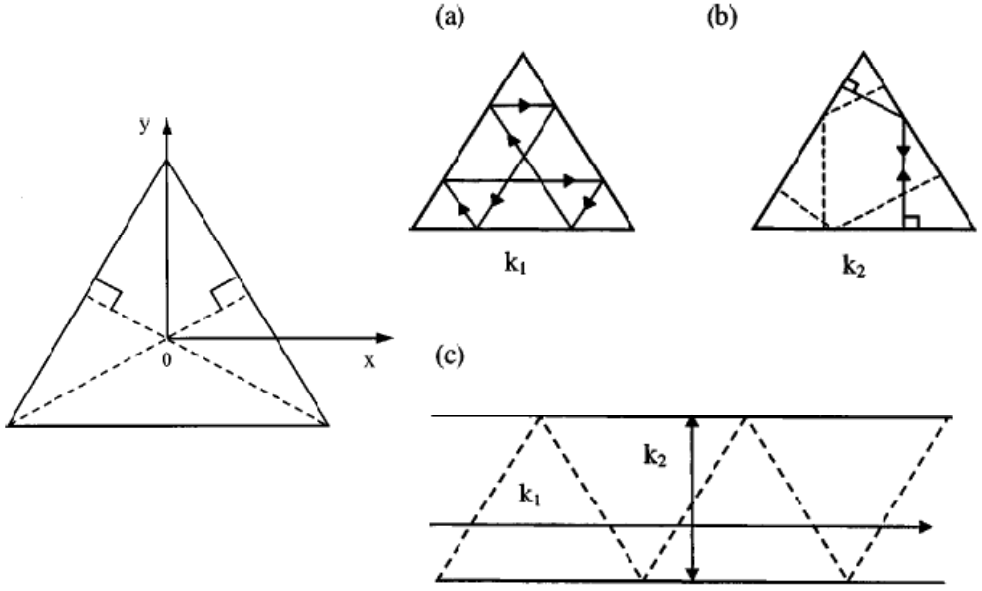

Wave vector $\boldsymbol{K}_2$; Wave function：

$$\sin(k_2y)$$

$$\sin\left[k_2\left(\frac{\sqrt{3}}{2}x+\frac{1}{2}y-\frac{a}{2\sqrt{3}}\right)\right]$$

$$\sin\left[k_2\left(\frac{\sqrt{3}}{2}x-\frac{1}{2}y+\frac{a}{2\sqrt{3}}\right)\right]$$

The boundary conditions

$$E_z(x,y)=0$$

nonvanishing solution：

$$k_1=\pm\frac{2m\pi}{3a},\quad m=1,2,3\ldots$$

$$k_2=\frac{2n\pi}{\sqrt{3}a},\quad n=1,2,3\ldots.$$

Physical Review A 62, 013816 (2000)

CL spectra and mode patterns of the equilateral-triangle cavities

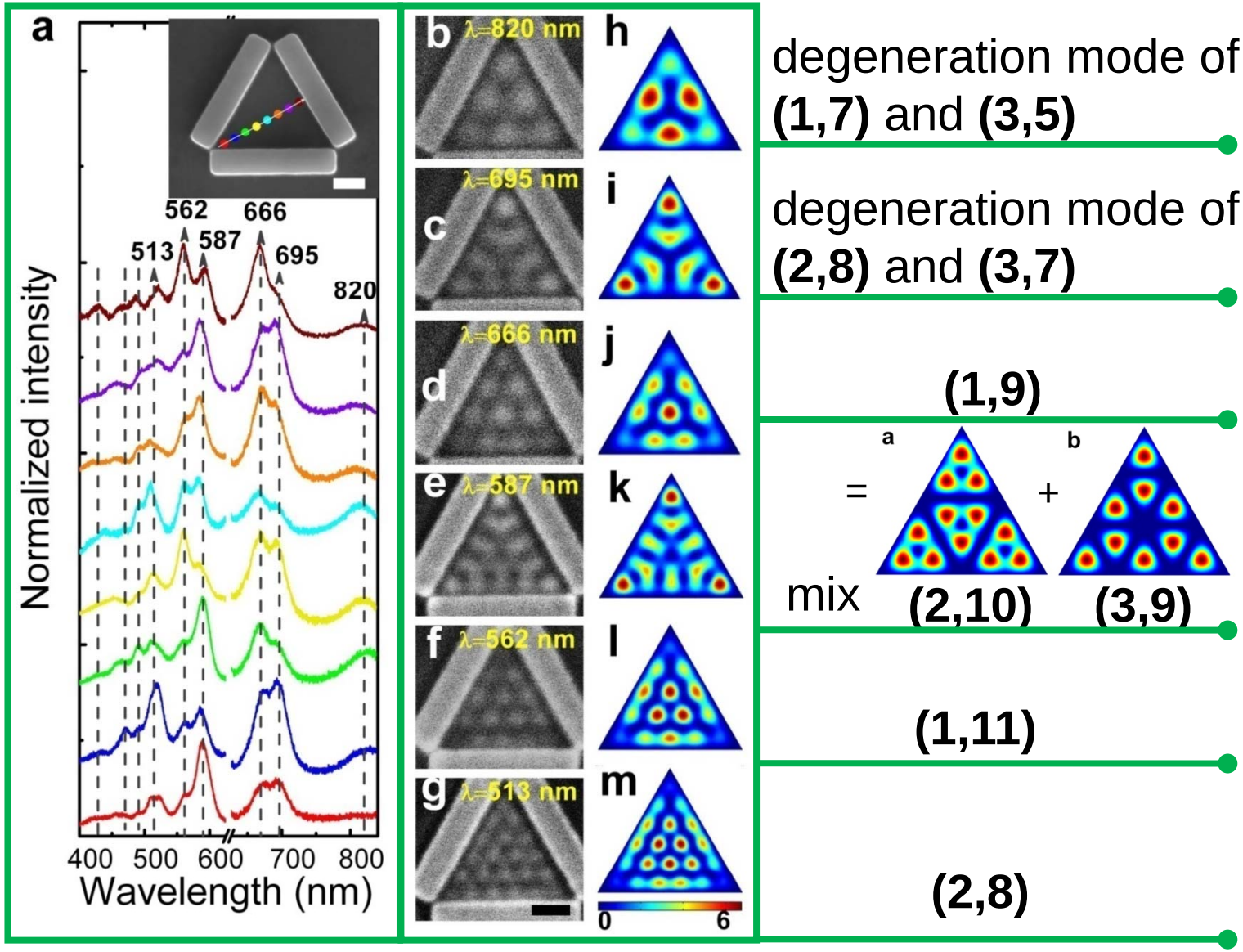

Xinli Zhu *et al*., DOI: 10.1002/adma.201001313

Comparison: Various fabrication method (tradition)

FIB milling

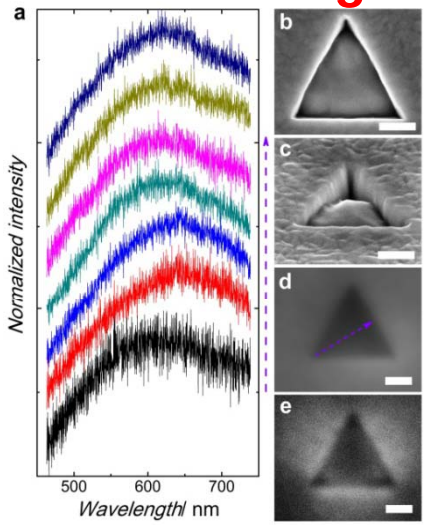

EBL/reative ion etching/MD

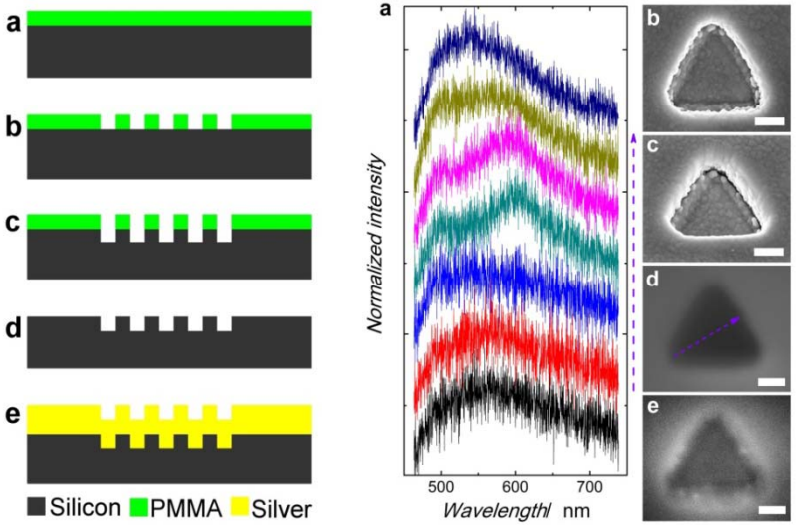

EBL/metal deposition

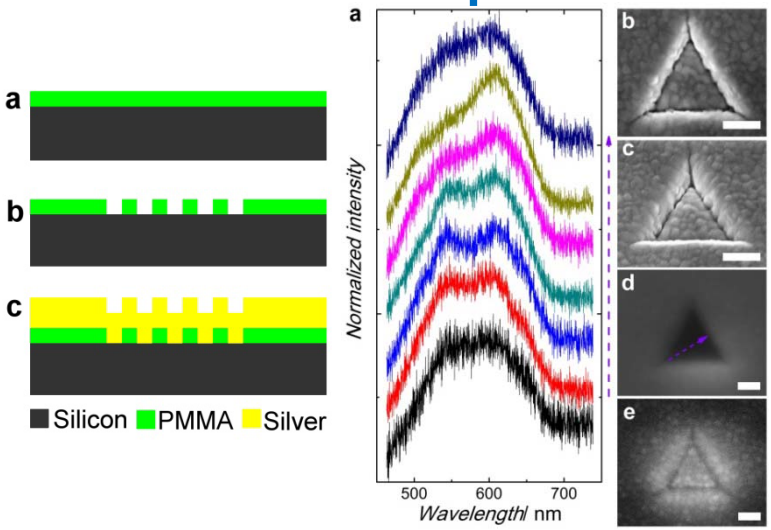

EBL/metal deposition/lift off

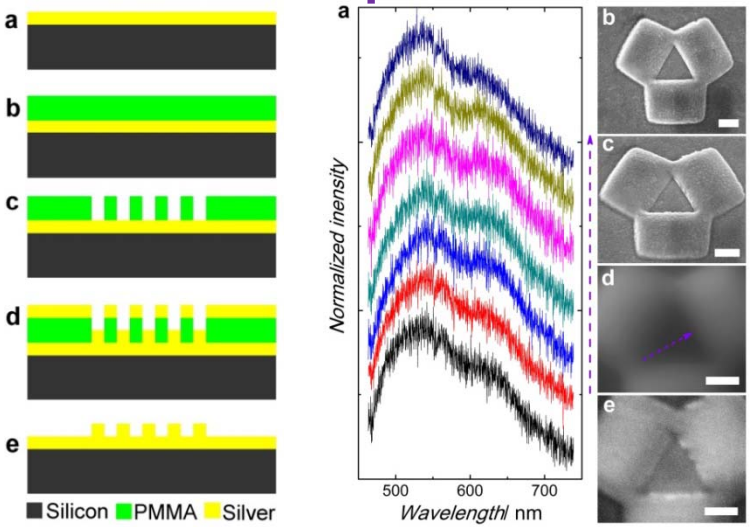

Our technique: different height

H=80 nm

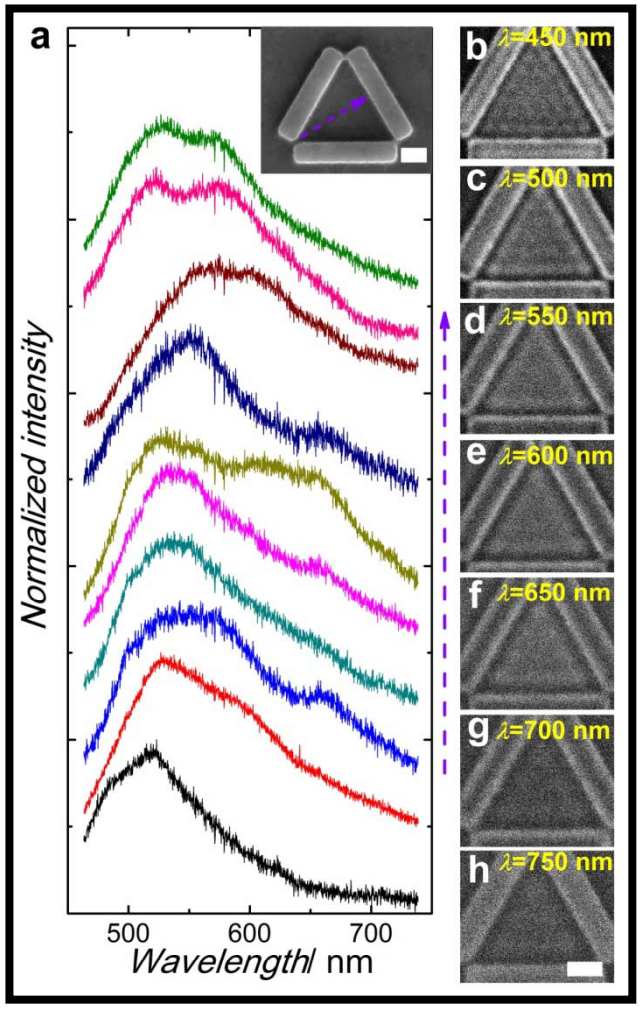

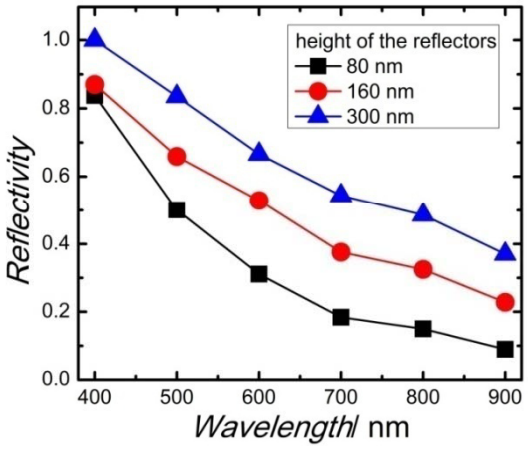

FDTD simulation

H=160 nm

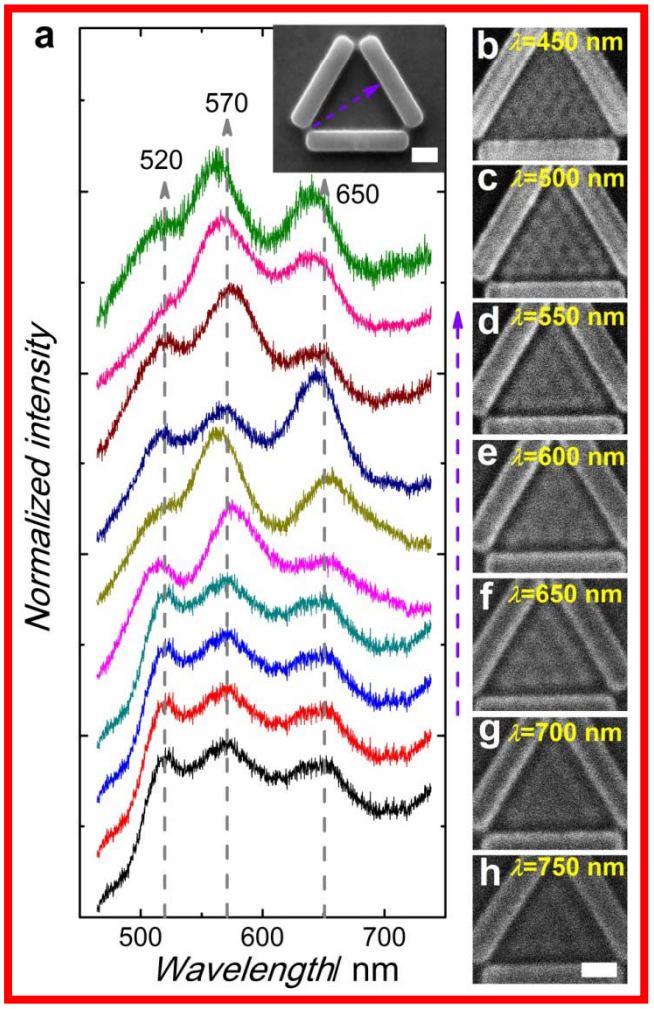

Conclusion

- The TS method combined with PMMA as a template was successfully used to create extraordinarily smooth metal nanostructures with a desirable feature size.

- The advantages of this method, including the high resolution, precipitous top-to-bottom profile with a high aspect ratio, and three-dimensional characteristics.

- The ultrasmooth surface and the large height of the metal reflectors are two indispensable factors to obtain clear resonant modes in the nanocavities.

科研经历和科研心得

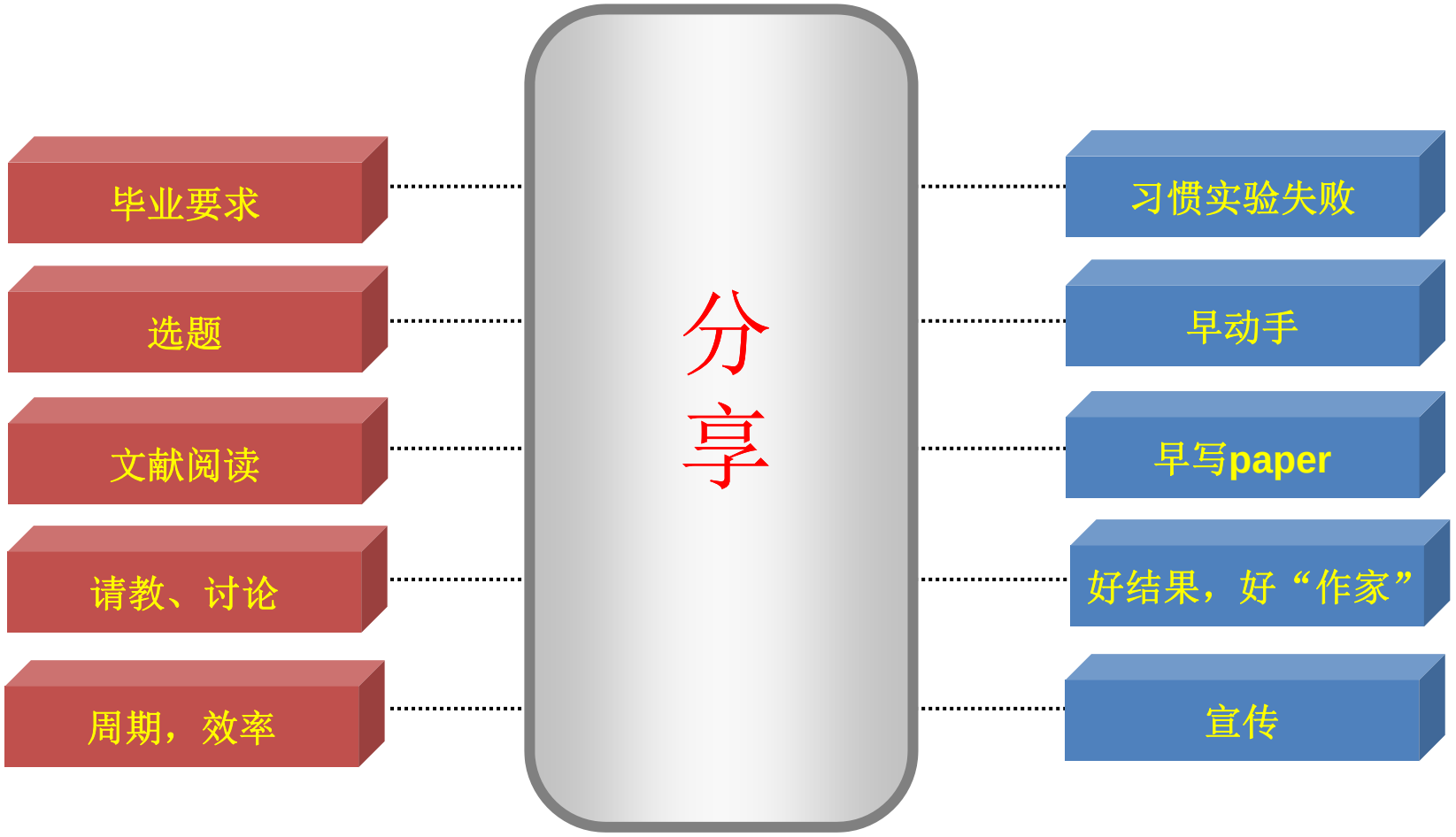

感谢

- 我的导师俞大鹏教授；
- 张家森教授的愉快合作；
- 电镜室徐军老师；
- 实验室的兄弟姐妹们。
- 科技部973计划
- 国家自然科学基金委
- 介观物理国家重点实验室自主科研项目
- 萃英论坛以及物理院研会


Thank you for attention.